Prion protein interaction with stress-inducible protein 1 enhances neuronal protein synthesis via mTOR

Martín Roffé[a], Flávio Henrique Beraldo[b], Romina Bester[c], Max Nunziante[c], Christian Bach[c], Gabriel Mancini[d,e], Sabine Gilch[c], Ina Vorberg[f], Beatriz A. Castilho[a], Vilma Regina Martins[d,e,1], and Glaucia Noeli Maroso Hajj[d,e,1,2]

[a]Departamento de Microbiologia, Imunologia e Parasitologia, Universidade Federal de São Paulo, 04023-062 São Paulo, Brazil; [b]J. Allyn Taylor Centre for Cell Biology, Molecular Brain Research Group, Robarts Research Institute, and Department of Physiology and Pharmacology, University of Western Ontario, London, ON, Canada N6A 5K8; [c]Institute of Virology, Technical University of Munich, 80333 Munich, Germany; [d]Ludwig Institute for Cancer Research, São Paulo Branch, 01323-903 São Paulo, Brazil; [e]Centro de Tratamento e Pesquisa A.C. Camargo, 01509-010 São Paulo, Brazil; and [f]Deutsches Zentrum für Neurodegenerative Erkrankungen, D-53175 Bonn, Germany

Edited by Charles Weissmann, Scripps Florida, Jupiter, FL, and approved June 8, 2010 (received for review January 28, 2010)

Transmissible spongiform encephalopathies are fatal neurodegenerative diseases caused by the conversion of prion protein (PrP^C) into an infectious isoform (PrP^{Sc}). How this event leads to pathology is not fully understood. Here we demonstrate that protein synthesis in neurons is enhanced via PrP^C interaction with stress-inducible protein 1 (STI1). We also show that neuroprotection and neuritogenesis mediated by PrP^C–STI1 engagement are dependent upon the increased protein synthesis mediated by PI3K-mTOR signaling. Strikingly, the translational stimulation mediated by PrP^C–STI1 binding is corrupted in neuronal cell lines persistently infected with PrP^{Sc}, as well as in primary cultured hippocampal neurons acutely exposed to PrP^{Sc}. Consistent with this, high levels of eukaryotic translation initiation factor 2α (eIF2α) phosphorylation were found in PrP^{Sc}-infected cells and in neurons acutely exposed to PrP^{Sc}. These data indicate that modulation of protein synthesis is critical for PrP^C–STI1 neurotrophic functions, and point to the impairment of this process during PrP^{Sc} infection as a possible contributor to neurodegeneration.

prion scrapie | neuritogenesis | neuroprotection | translation initiation | neurotrophic factors

Prion protein (PrP^C) is a major component in the physiopathology of transmissible spongiform encephalopathies. PrP^C can be converted to an infectious isoform (PrP^{Sc}), the accumulation of which eventually leads to neurodegeneration (1). Current debate has focused on whether the toxic PrP^{Sc} aggregates themselves are the cause of neuronal cell death, or whether modifications in PrP^C structure lead to the loss of its functions explaining the pathogenesis of these diseases (1, 2).

PrP^C has been shown to mediate neuroprotection against cellular and systemic insults, neuritogenesis, neuronal plasticity and excitability, and memory formation and consolidation (2). Although posttranslational modifications can modulate short-term neuronal plasticity, long-term plastic changes and memory consolidation require de novo protein synthesis. Control of protein synthesis by neurotrophic factors is involved both in neuronal development, for example in growth cone guidance, and in nervous system function, as part of processes such as long-lasting synaptic plasticity (3, 4). Despite their mutual involvement in multiple neuronal processes, the link between PrP^C and protein synthesis has not been addressed.

The rate of translation is primarily regulated at the initiation phase, which involves the association of the small ribosomal subunit with the mRNA and the scanning of the message for the initiator AUG codon. Among the targets of translational control is the assembly, on the mRNA 5′ cap structure, of the eIF4F complex, comprising the cap-binding protein eIF4E, the helicase eIF4A and the scaffold protein eIF4G (5). The latter then mediates the recruitment of the 43S preinitiation complex, composed of the 40S subunit, the ternary complex eIF2–GTP-initiator tRNA, and other initiation factors. eIF4E-binding proteins (4E-BPs) act as negative regulators of translation by sequestering eIF4E thus hampering the formation of eIF4F. Phosphorylation of 4E-BPs leads to their dissociation from eIF4E, thus increasing the rate of translation (5, 6). 4E-BPs are directly phosphorylated by the mammalian target of rapamycin complex 1 (mTORC1), which is activated in response to extracellular stimuli through, for example, the phosphoinositide 3-kinase (PI3K)–Akt signaling pathway (6). mTORC1 also targets the p70S6 kinase (p70S6K), which activates the ribosomal protein S6 (7) and initiation factors either directly, such as eIF4B (8), or indirectly, such as eIF4A (9), correlating with increased protein synthesis in neurons (10, 11). Another regulatory step of translation initiation involves the phosphorylation of the alpha subunit of eukaryotic translation initiation factor 2 (eIF2α), resulting in translation inhibition by blocking the activity of the guanine nucleotide exchange factor eIF2B (5). These regulatory pathways have previously been implicated in nervous system development and brain functions (6). For example, animals devoid of 4E-BP2 or the eIF2α kinase GCN2 exhibit a lower threshold for late long-term potentiation induction and impaired hippocampus-dependent memory (12, 13).

Many of the neurotrophic functions of PrP^C have been attributed to its ability to bind and/or modulate the activity of several ligands (14). In particular, PrP^C binding to the astrocyte-secreted stress-inducible protein 1 (STI1) (15) induces neuronal survival, neuritogenesis, and memory formation and consolidation (16, 17). Here we show that STI1 increases PrP^C-dependent neuronal protein synthesis via the PI3K–Akt–mTOR and ERK1/2 pathways, and that this process is essential to the neurotrophic activities of PrP^C. Finally, we demonstrate that protein synthesis is partially impaired in PrP^{Sc}-infected cells, correlating with increased eIF2α phosphorylation. Our results suggest that the PrP^C–STI1 interaction modulates the pool of cellular proteins needed for proper neuronal function, and that prion infection may corrupt PrP^C–STI1 functions dependent on new protein synthesis, as well as cellular responses to other neurotrophic factors.

Results

PrP^C Interaction with STI1 Up-Regulates Neuronal Protein Synthesis. To address whether PrP^C association with STI1 directly regulates protein synthesis, hippocampal neurons were metabolically labeled with [^{35}S]-methionine. WT neurons ($Prnp^{+/+}$) exhibited a dose-dependent increase in protein synthesis upon STI1 treat-

Author contributions: M.R., I.V., B.A.C., V.R.M., and G.N.M.H. designed research; M.R., F.H.B., R.B., M.N., C.B., G.M., and G.N.M.H. performed research; M.R., V.R.M., and G.N.M.H. analyzed data; R.R., M.N., C.B., S.G., I.V., and B.A.C. contributed new reagents/analytic tools; and M.R., M.N., I.V., B.A.C., V.R.M., and G.N.M.H. wrote the paper.

The authors declare no conflict of interest.

This article is a PNAS Direct Submission.

[1]G.N.M.H. and V.R.M. contributed equally to this work.

[2]To whom correspondence should be addressed. E-mail: ghajj@bcm.ludwig.org.br.

This article contains supporting information online at www.pnas.org/lookup/suppl/doi:10.1073/pnas.1000784107/-/DCSupplemental.

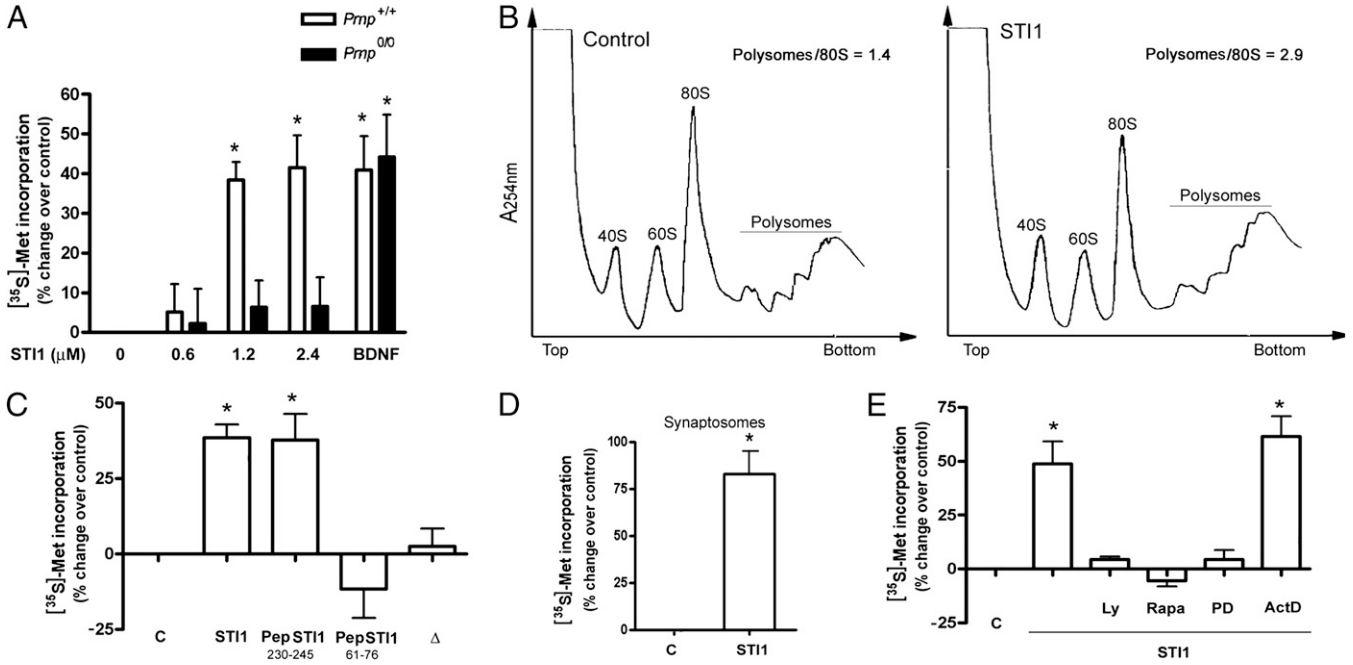

Fig. 1. STI1–PrP^C interaction enhances protein synthesis in a PI3K-mTOR and ERK1/2 dependent manner. (*A*) *Prnp*$^{+/+}$ (open bars) or *Prnp*$^{0/0}$ (filled bars) neurons were incubated with [^{35}S]-methionine, followed by stimulation with STI1 or 100 ng/mL BDNF for 30 min. Graph shows percentage of increase of [^{35}S]-methionine incorporation relative to control cells. (*B*) Polysome profiles from neurons without treatment (control, *Left*) or treated with 2.4 μM STI1 for 30 min (*Right*). (*C*) Neurons were incubated with 2.4 μM STI1, 80 μM PepSTI1$_{230–245}$, 80μM PepSTI1$_{61–76}$, or 2.4 μM STI1Δ(Δ). Graph shows percentage change of [^{35}S]-methionine incorporation relative to control cells. (*D*) Synaptosomes were treated with 2.4 μM STI1 for 30 min. Graph shows percentage of increase of [^{35}S]-methionine incorporation relative to control. (*E*) Neurons were preincubated with Ly294002 (5 μM, Ly), rapamycin (20 nM, Rapa), PD98059 (50 μM, PD), or Actinomycin D (1.5 μM, ActD) for 15 min before addition of 2.4 μM STI1. Graph shows percentage of increase of [^{35}S]-methionine incorporation relative to untreated cells. (*A, C,* and *E*) *$P < 0.05$, ANOVA followed by Tukey post hoc test. (*D*) *$P < 0.05$, Student *t* test.

ment. PrP^C-null neurons (*Prnp*$^{0/0}$, Fig. 1*A*) did not present any response to STI1, whereas protein synthesis induced by BDNF was equivalent in both cell types, indicating that STI1 signaling is dependent on PrP^C and that PrP^C-null cells can respond with increased protein synthesis to other neurotrophic stimuli (Fig. 1*A*). The effect of PrP^C–STI1 on translation initiation levels was then evaluated by polysome profile analysis (Fig. 1*B*). Untreated neurons show a polysomes/monosome ratio of 1.4, whereas neurons treated with STI1 showed a polysomes/monosome ratio of 2.9, reflecting a reduction in the amount of free ribosomes and a concomitant increase in the number of actively translating ribosomes. The requirement of STI1-PrP^C interaction for protein synthesis was further confirmed by the positive effect of treatment with the STI1 peptide that comprises the PrP^C-binding site (Pep STI1$_{230–245}$), whereas an STI1 peptide from a different region (PepSTI1$_{61–76}$), used as a control, had no effect (Fig. 1*C*). In addition, no alteration in protein synthesis was observed in the presence of an STI1 deletion mutant lacking the PrP^C-binding site (Δ, Fig. 1*C*). These results suggest that PrP^C–STI1 interaction stimulates translation initiation increasing protein synthesis.

The STI1-induced increase in protein synthesis was also observed in synaptosomes, suggesting that STI1 may also affect local translation at synapses, and indicates that STI1 increases the translation of preformed mRNAs (Fig. 1*D*).

PI3K–mTOR and ERK1/2 Pathways Mediate Protein Synthesis Stimulation by PrP^C–STI1 Binding. To study the signaling pathways activated by the PrP^C–STI1 interaction leading to increased protein synthesis, hippocampal neurons were pretreated with a set of specific inhibitors and labeled with [^{35}S]-methionine in the presence of STI1 (Fig. 1*E*). LY294002, rapamycin, and PD98059, which are inhibitors of PI3K, mTORC1, and ERK1/2, respectively, abolished STI1-induced protein synthesis. On the other hand, addition of actinomycin D did not alter the increase in [^{35}S]-methionine incorporation mediated by PrP^C–STI1, demonstrating that this effect was independent of transcription (Fig. 1*E*).

We next evaluated the phosphorylation of the immediate downstream targets in the PI3K–Akt–mTOR pathway in response to PrP^C–STI1. STI1 treatment promoted rapid phosphorylation of Akt, peaking at 1 min in WT cells, whereas no effect was observed in PrP^C-null cells (Fig. 2*A*). Consistent with mTOR activation, a peak of p70S6K phosphorylation was observed in WT neurons after 10–15 min of STI1 treatment. However, no increase in p70S6K phosphorylation was observed in PrP^C-null cells or in WT neurons treated with the STI1 deletion mutant (Δ, Fig. 2*B*). Confirming these results, preincubation with LY294002 or rapamycin abolished p70S6K phosphorylation stimulated by PrP^C–STI1 interaction (Fig. 2*B*). PrP^C-null neurons responded with p70S6K phosphorylation upon BDNF stimulation, demonstrating that this pathway is not compromised in these cells (Fig. S1*A*). Other targets of mTORC1 are the three members of the 4E-BPs family (4E-BP1, 4E-BP2, and 4E-BP3) (5). Hippocampal neurons express low levels of 4E-BP1 compared with astrocytes, whereas 4E-BP2 was highly expressed in neurons (12) (Fig. S1*B*). To detect neuronal 4E-BP2 phosphorylation, we used an antibody directed against 4E-BP1 phosphorylated at T37/46, which cross-reacts with 4E-BP2 when phosphorylated at the equivalent sites. 4E-BP1 and 4E-BP2 can be distinguished based on their different migration when subjected to 12% SDS/PAGE. Stimulation with STI1 for 30 min did not affect 4E-BP2 expression (Fig. S1*C*). However, STI1 treatment resulted in an increase in 4E-BP2 phosphorylation in WT neurons, but not in PrP^C-null neurons (Fig. 2*C*).

We have previously determined that the PrP^C–STI1 interaction triggers ERK1/2 activation (17). The translation initiation factor eIF4E is directly phosphorylated at S209 by the MAPK interacting kinases (Mnk1 and Mnk2) (18). Hippocampal neu-

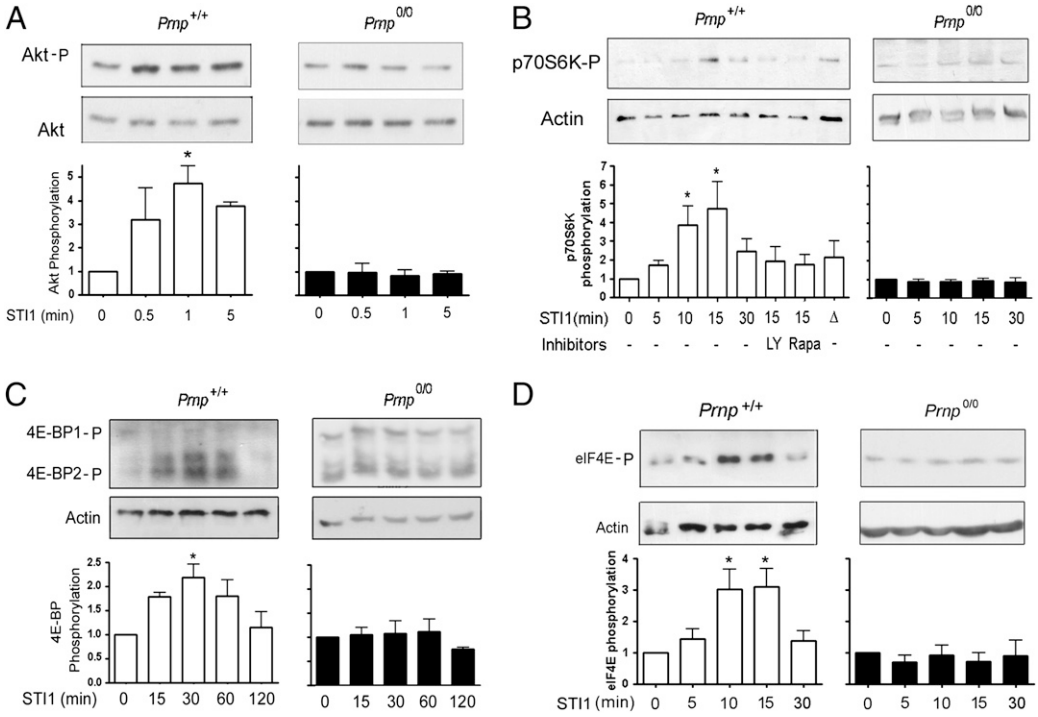

Fig. 2. STI1–PrP^C interaction induces phosphorylation of Akt, p70S6K, 4E-BP2, and eIF4E. *Prnp*$^{+/+}$ (open bars) or *Prnp*$^{0/0}$ (filled bars) neurons were treated with 2.4 μM STI1 or STI1Δ(Δ) for the indicated times. Western blots were performed for (*A*) phospho-Akt and total-Akt, (*B*) phospho-p70S6K and actin, (*C*) phospho-4E-BP1 and actin, and (*D*) phospho-eIF4E and actin. All values are expressed relative to control. Where indicated, cells were preincubated for 1 h with Ly294002 (5 μM, Ly) or rapamycin (20 nM, Rapa). *$P < 0.05$, ANOVA followed by Tukey post hoc test.

rons from WT mice showed a peak of eIF4E phosphorylation after 10–15 min of STI1 treatment, whereas no effect was observed in PrP^C-null neurons (Fig. 2*D*).

These data, taken together, indicate that PrP^C–STI1 interaction promotes protein synthesis and mTORC1 activity, correlating with increased Akt, p70S6K, and 4E-BP2 phosphorylation.

Neuritogenesis and Neuroprotection Induced by PrP^C–STI1 Are Mediated by the PI3K–mTOR Pathway. The PI3K–mTOR pathway is important for neuronal processes such as those elicited by neurotrophic factors (19). In WT hippocampal neurons, PrP^C–STI1 binding modulates neuritogenesis by increasing the number of cells with neurites, as well as the number of cells with neurites longer than 30 μm (Fig. 3 *A–D* and Fig. S2), whereas the neurite length and the number of neurites per cell remained unchanged (Fig. S3*A–D*). Pretreatment of neurons with LY294002 (Fig. 3 *A* and *B* and Fig. S2) or rapamycin (Fig. 3 *C* and *D* and Fig. S2) abrogated PrP^C–STI1–dependent neuritogenic effects, demonstrating the involvement of the PI3K–mTOR pathway in these phenotypes. Neither STI1 nor the inhibitors had any effect on PrP^C-null neurons (Fig. S3 *E–H*).

PrP^C–STI1 interaction also results in neuroprotection against cell death induced by staurosporine (17). Here we show that neuroprotection was also impaired when neuronal cultures were exposed to LY294002 or rapamycin before STI1 treatment (Fig. 3*E*). Only conditions in which the treatments with inhibitors alone did not increase cell death were used. These results suggest that both neuritogenesis and neuroprotection induced by PrP^C–STI1 binding use the PI3K-mTOR pathway, and that protein synthesis is a key step for PrP^C–STI1–induced neurotrophic effects.

Protein Synthesis Is Corrupted in PrP^{Sc}-Infected Cells. The N2a and SN-56 neuronal cell lines persistently infected with the 22L PrP^{Sc} strain were used to determine whether PrP^{Sc} infection alters protein synthesis. Before use in the experiments, all N2a and SN-56 cells were checked for the presence of proteinase K (PK)–resistant PrP^{Sc}. Persistently infected N2a cells were [^{35}S]-methionine labeled in the presence or absence of recombinant STI1. Protein synthesis in unstimulated 22L-infected cells was reduced by 36.0 ± 0.7% when compared with mock-infected cells (Fig. 4*A*), indicating that PrP^{Sc} infection reduced levels of translation. Mock-infected cells responded with an increase in protein synthesis upon STI1 (36.4 ± 2.0%) or insulin (36.9 ± 8.7%) treatment. In 22L-infected cells, we observed a small response to STI1 and insulin, which was not statistically significantly different from untreated 22L-infected cells (Fig. 4*A*). The same response was observed in persistently 22L-infected SN-56 cells, in which there is a reduction to 51.2 ± 2.0% in comparison with mock-infected cells. The 22L-infected cells also did not demonstrate significant induction in protein synthesis by STI1 or insulin (Fig. 4*B*).

To understand how primary cultures respond to PrP^{Sc} exposure, we incubated hippocampal neurons with mock-infected or 22L-infected brain extracts. Three days after exposure, we observed neurons that exhibited guanidinium-resistant PrP^{Sc} deposits (Fig. S4*A*). These 22L-exposed neurons were also positive for PK-resistant PrP^{Sc} molecules (Fig. S4*B*). 22L-exposed neurons showed a 30 ± 2% reduction in protein synthesis compared with unstimulated mock-infected neurons (Fig. 4*C*). Similar to what has been observed for N2a-infected cells, primary cultures exposed to 22L brain extract presented a small and nonstatistically significant response to STI1 and insulin when compared with mock-infected cells (Fig. 4*C*). Taken together, these data indicate that PrP^{Sc} infection leads to a reduction of protein synthesis and to an impaired response to the factors tested here.

PrP^{Sc} Infection Increases the Phosphorylation of eIF2α. PrP^{Sc} infection has previously been associated with ER stress (20). The hallmark of ER stress is the activation of PKR-like endoplasmic reticulum kinase (PERK), resulting in eIF2α phosphorylation, which in turn inhibits global protein synthesis. Another eIF2α kinase, double-

NEUROSCIENCE

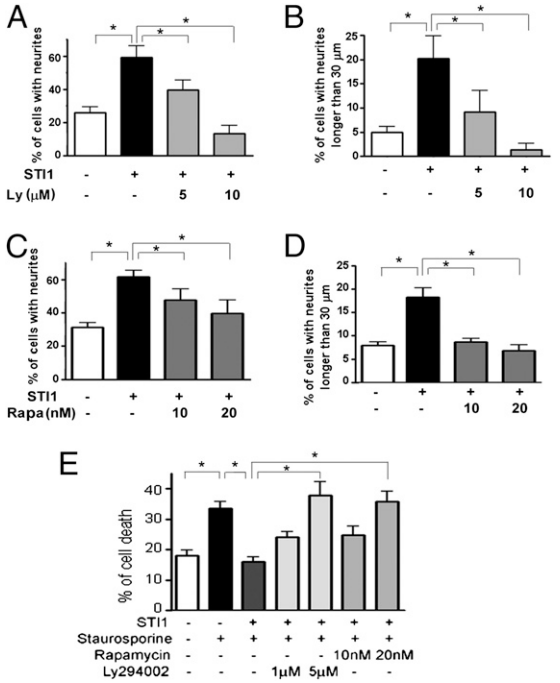

Fig. 3. PrP^{C}–STI1–induced neuritogenesis and neuroprotection is dependent on PI3K and mTOR signaling. Neurons were cultured with 0.6 μM STI1 and Ly294002 (*A* and *B*) or STI1 and rapamycin (*C* and *D*) for 24 h. Morphometric quantification of the following parameters was performed: percentage of cells with neurites (*A* and *C*), percentage of cells with neurites longer than 30 μm (*B* and *D*). (*E*) Neurons were cultured with 1.2 μM STI1 and Ly294002 or rapamycin for 1 h, followed by addition of 25 nM staurosporine. After 24 h, cells were fixed and stained with propidium iodide. Graph shows the percentage of pyknotic cells. *$P < 0.05$, ANOVA followed by Tukey post hoc test.

stranded RNA-activated protein kinase (PKR), typically activated by dsRNA, can also be activated by Rax/PACT in response to several cellular stresses (21). In N2a cells infected with PrP^{Sc}, eIF2α phosphorylation levels were 2.5 ± 0.4 times higher than in mock-infected cells (Fig. 5*A*). This phosphorylation remained high even after STI1 treatment (Fig. 5*A*). Tunicamycin, an ER stress inducer, increased the levels of eIF2α phosphorylation in mock-infected cells, but not in PrP^{Sc}-infected cells (Fig. 5*A*), consistent with a prior establishment of ER stress. We also observed increased levels of phosphorylated PKR, indicative of PKR activation (Fig. 5*B*). 22L-infected SN-56 cells also displayed increased eIF2α phosphorylation (Fig. 5*C*). Because PrP^{C} ligands such as the 37-kDa laminin receptor have been demonstrated to influence PrP^{Sc} conversion (22), we checked whether STI1 could alter PrP^{Sc} amounts. Levels of PK-resistant PrP^{Sc} were not affected by STI1 or PepSTI1$_{230–245}$ treatment (Fig. S5).

In primary neurons acutely exposed to PrP^{Sc}-infected brain extract, we also observed increased levels of eIF2α phosphorylation (Fig. 5*D*). Together, these results indicate that the elevated levels of eIF2α phosphorylation in PrP^{Sc}-infected cells could be a major contributor for the reduced rates of protein synthesis in these cells and their failure to respond to STI1 and insulin.

Discussion

This work is unique in describing the involvement of prion protein in the control of protein synthesis in both physiological and pathological conditions. Our results show that the PrP^{C}–STI1 interaction activates protein synthesis through the PI3K–Akt–mTOR and ERK1/2 pathways.

The mTOR pathway is essential for the response to neurotrophic factors, protection against cell death, neuronal plasticity,

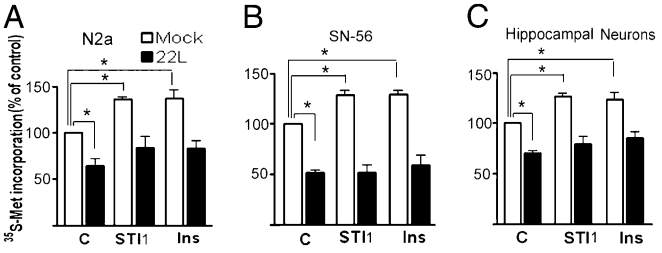

Fig. 4. Protein synthesis is partially impaired in PrP^{Sc}-infected cells. Mock (open bars) or 22L persistently infected (filled bars) N2a (*A*) or SN-56 (*B*) cells were preincubated with [^{35}S]-methionine, followed by 2.4 μM STI1 or 5 μg/mL insulin stimulation for 30 min. Graph shows the percentage of [^{35}S]-methionine incorporation relative to mock-infected cells. (*C*) Primary neurons exposed to mock (open bars) or 22L-infected (filled bars) brain extracts were preincubated with [^{35}S]-methionine, followed by 2.4 μM STI1 or 5 μg/mL insulin for 30 min. Graph shows percentage of [^{35}S]-methionine incorporation relative to untreated, mock-infected cells. *$P < 0.05$, ANOVA followed by Tukey post hoc test.

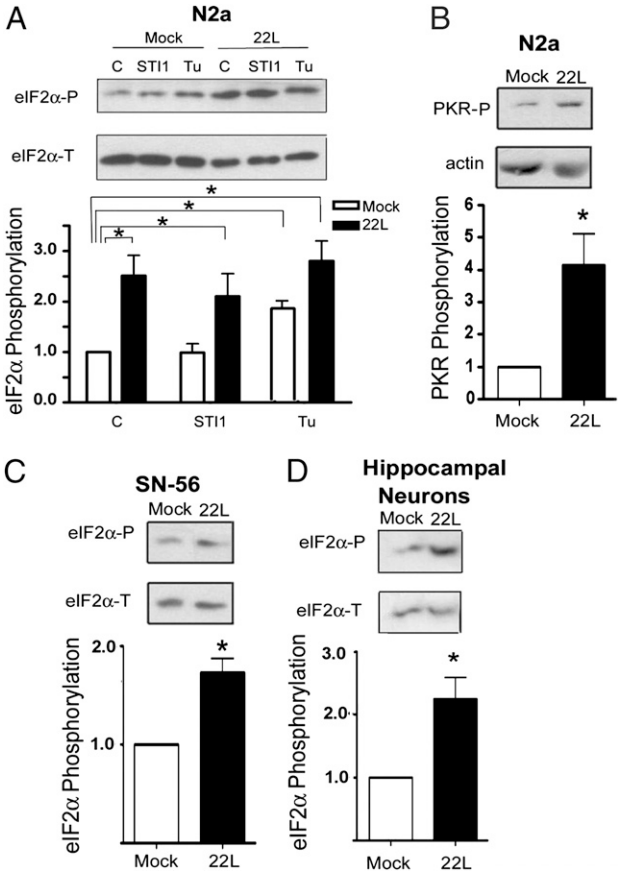

Fig. 5. PrP^{Sc} infection leads to eIF2α phosphorylation. Mock-infected (open bars) or 22L-infected N2a (filled bars) were treated with 2.4 μM STI1 or 2.5 μg/mL tunicamycin (Tu) for 1 h. Western blots were performed for antiphosphorylated and total eIF2α (*A*), phospho-PKR and actin (*B*). Graphs show levels of phospho-eIF2α (*A*) or phospho-PKR (*B*) relative to control. (*C*) Mock-infected (open bars) or 22L–persistently infected SN-56 cells (filled bars) were subjected to Western blot with antiphosphorylated or total eIF2α. Graph shows levels of phospho-eIF2α relative to control. (*D*) Hippocampal neurons were exposed to mock (open bars) or 22L-infected brain extract (filled bars) and subjected to Western blot with antiphosphorylated or total eIF2α. Graph shows levels of phospho-eIF2α relative to control. (*A*) *$P < 0.05$, ANOVA followed by Tukey post hoc test. (*B–D*) *$P < 0.05$, Student *t* test.

and memory consolidation (19). 4E-BPs, when phosphorylated by mTORC1, release eIF4E, allowing its association with eIF4G, thus directly de-repressing translation initiation (5). Importantly, 4E-BPs have been implicated in memory consolidation (12) and growth cone guidance (23). Phosphorylation of another mTORC1 target, p70S6K, has been correlated with increased translation in a variety of experimental models (7). Even though the mechanism of action is still under discussion, it is known that p70S6K has multiple targets among the translational machinery, such as the ribosomal protein S6, eIF4B, and eEF2 kinase (6) (Fig. S6). Consistent with the increased translation rates induced by STI1 observed by methionine incorporation and polysome profiles, we found that these two direct targets of mTOR, 4E-BP2 and p70S6K, were phosphorylated in response to PrP^C–STI1 binding. We also show that eIF4E phosphorylation is stimulated by PrP^C–STI1 engagement, possibly as a result of the activation of the ERK1/2 pathway and its downstream effectors Mnk1 and Mnk2 (18) (Fig. S6). Even though a direct effect of p70S6K and eIF4E on general protein synthesis is not clear, their phosphorylation is intimately associated with neuronal stimuli that increase protein synthesis, and it is possible that these events may favor the translation of a specific subset of mRNAs related to neuronal survival and differentiation. In fact, recent work has demonstrated that p70S6K up-regulates the translation of collapsing response mediator protein 2 and Tau in axons, inducing the formation of multiple axons (24), and that eIF4E phosphorylation increases mRNA translation of the antiapoptotic protein MCL-1 (25).

It is interesting that PI3K-mTOR and ERK1/2 pathways cross-talk. ERK1/2 was shown to activate translation through 90 kDa ribosomal S6 kinase 1 (RSK1). RSK1 phosphorylates and inactivates tuberous sclerosis 2, thereby promoting mTOR signaling and translation (26). Furthermore, RSK1 directly phosphorylates eIF4B to promote cap-dependent translation (27). By binding to PrP^C, STI1 stimulates both ERK1/2 and PI3K and induces protein synthesis. Because the inhibitors of both pathways almost completely blocked protein synthesis induced by STI1, we believe that the most important STI1 effects arise from the cross-talk between PI3K and ERK1/2 pathways (Fig. S6).

Our data also suggest that an increase in protein synthesis is a key step in PrP^C–STI1–dependent neuronal differentiation. PrP^C is located in lipid rafts (2), and activated Akt targeted to these structures mediates axonal branching via mTOR (28), implying that the STI1–PrP^C induction of mTOR activation may occur in lipid rafts. The present data also point to a dependence on PI3K-mTOR activation by PrP^C–STI1 for neuroprotection. Neuroprotection may involve the translation of a different subset of proteins in a PI3K and mTOR-dependent manner, such as Engrailed (a transcription factor essential to dopaminergic neuron survival) (29) or the antiapoptotic protein B-cell CLL/lymphoma 2 (Bcl-2) (30). Protein kinase A (PKA) is essential to the neuroprotective functions of PrP^C–STI1 (17). PKA and mTOR pathways can also cooperate to promote survival. For example, the transcription factor CREB, which is directly activated by PKA, promotes Bcl-2 transcription, mediating the antiapoptotic effects of cAMP (31). Interestingly, the p85 subunit of PI3K is phosphorylated by PKA both in vitro and in vivo, which increases PI3K activity (32).

There is increasing evidence supporting the notion that fine tuning of neuronal translation, such as that elicited by neurotrophic factors in synapses, underlies many neuronal processes (33, 34). Major components of the protein synthesis machinery are found in axons, dendrites, and dendritic spines, and localized regulation of translation has been implicated in long-term potentiation and long-term depression (35). It has been demonstrated that β-actin (23) and even CREB (36) mRNAs, are specifically translated at the growth cones. The fact that STI1 stimulates protein synthesis in synaptosomes suggests that PrP^C–STI1 modulates local translation, consistent with roles in memory consolidation and synaptic plasticity. Interestingly, PrP^C KO animals have been demonstrated to have higher sensitivity to different agents that cause neuronal injury (2, 14), including hypoxia (37), and an important part of the hypoxia response is mediated through the mTOR pathway (38).

The present data demonstrate that protein synthesis is partially inhibited in PrP^{Sc}-infected neurons. eIF2α phosphorylation is known to repress translation at the initiation stage (5). Consistent with this, we found higher levels of phosphorylated eIF2α in PrP^{Sc}-infected cells and in neurons acutely exposed to brain extracts from PrP^{Sc}-infected mice, used here to mimic the microenvironment that a neuron would be exposed during infection. This would indicate that eIF2α phosphorylation is one of the first cellular signs of the disease. The fact that the response to insulin, as well as to STI1, was compromised in these cells suggests that by blocking protein synthesis, PrP^{Sc} infection may impair the general and/or local mRNA translation activated by neurotrophic signals. We could not exclude a failure in PI3K-mTOR and ERK1/2 pathway activation due to the conversion of PrP^C into PrP^{Sc}, which could contribute to the impairment in protein synthesis.

We observed that one of the eIF2 kinases, PKR, is phosphorylated and thus active, in infected cells. Expression of cytosolic PrP^C has also been shown to activate PKR (39), and neuronal immunostaining for activated PKR has been found in cases of Creuztfeldt-Jakob disease (40). Interestingly, phosphorylated PKR is also a marker for cognitive decline in individuals with Alzheimer's disease (41) and, in cultured neurons, PKR activation and eIF2α phosphorylation play a role in the induction of apoptosis by β-amyloid peptides (42).

In conclusion, we have demonstrated an important function for PrP^C in regulating protein synthesis in neurons upon binding to the neurotrophic-like factor STI1. We showed that protein synthesis stimulation by STI1 and other neurotrophic factors is impaired in PrP^{Sc}-infected cells. The impaired response of PrP^{Sc}-infected neurons, because of alterations either on normal PrP^C or on the downstream cellular signaling, may lead to compromised neuronal functions found in transmissible spongiform encephalopathies. Our results suggest that therapeutic strategies directed to relieve the inhibition of protein synthesis promoted by eIF2α phosphorylation and/or to stimulate mTOR/ERK1/2 pathways would be a valuable approach for prion and other neurodegenerative diseases.

Methods

Proteins, Peptides, Inhibitors, and Antibodies. Murine His_6-STI1 (STI1) and His_6-STI1(Δ) with the PrP^C binding site deleted (amino acids 230–245), were purified as described (17). Peptides corresponding to the murine STI1 amino acid sequence were as follows: 230-ELGNDAYKKKDFDKAL-245 ($PepSTI_{230–245}$) and 61-GCKTVDLKPDWGKGYS-76 ($PepSTI_{61–76}$) (Neosystem and Genescript). Inhibitors were as follows: PD98059, LY294002, staurosporine (all from Calbiochem), and rapamycin (Sigma). Antibodies were the following: rabbit anti–phospho-T421/S424-p70S6K, rabbit anti–phospho-S209-eIF4E, rabbit anti–phospho-T308-Akt, rabbit anti–phospho-T37/46–4E-BP1, and rabbit anti–4E-BP2 (all from Cell Signaling Technology), mouse anti-actin (Sigma), rabbit anti–phospho-S51-eIF2α, and mouse anti–eIF2α (both from BioSource), anti–phospho-T446-PKR (Abcam), and anti-PrP^C (4H11) (43), peroxidase anti-mouse, and anti-rabbit IgG (Amersham Biosciences).

Neuronal Cell Culture. Hippocampal neurons were obtained from embryonic day 17 (E17) mice as described elsewhere (17). N2a and SN-56 cells were cultured in DMEM containing 10% FCS.

Synaptosome Preparation. Procedural details can be found in *SI Text.* Briefly, dissected cortex from adult mice was homogenized in isotonic buffer. The homogenate was sequentially filtered through 100-μm and 5-μm membranes. The final filtrate was centrifuged, and the pellet was used immediately.

Metabolic Labeling with [^{35}S]-Methionine. Procedures are detailed in *SI Text.* [^{35}S]-Met was added to cells 15 min before treatment, and cells were treated with STI1, STI1Δ, $PepSTI1_{230–245}$, or $PepSTI1_{61–76}$ for 30 min. When inhibitors were used, they were incubated along with [^{35}S]-Met for 15 min, followed by STI1 for 30 min. Synaptosomes were prewarmed at 37 °C for 10 min in the presence of [^{35}S]-Met, followed by STI1 treatment for 30 min. Cells or synaptosomes were lysed and spotted onto filter paper. Nonincorporated

amino acids were removed by trichloroacetic acid washing. Radioactivity was measured by scintillation counting.

Polysome Profiles. Detailed procedures can be found in *SI Text*. Briefly, neurons were treated with STI1 for 30 min. Cell extracts were subjected to a linear 7–47% sucrose gradient. Absorbance at 254 nm was detected in a continuous flow. Quantification was performed by measuring the area under the peak of 80S and the polysomes and calculating the polysomes/monosome ratio.

Immunoblotting. Cells (10^6) were treated with STI1 or Δ, or preincubated for 1 h with Ly294002 or rapamycin before STI1 addition. Western blots were performed against phospho-Akt, phospho-p70S6K, phospho-eIF4E, phospho-eIF2α, phospho-T37/46–4E-BP1, or phospho-PKR. Membranes were reprobed with antibodies against Akt, eIF2α, or actin. Densitometric scanning and analysis were performed using Scion Image software. Values represent the ratio between levels of phospho-Akt/Akt, phospho-p70S6K/actin, phospho-4E-BP1/actin, phospho-eIF4E/actin, or phospho-eIF2α/eIF2α. Untreated cell values were set as 1.0, and all other values shown are relative to this value.

Neuritogenesis Assay. Cells were pretreated with signaling inhibitors followed by treatment with 0.6 μM STI1 for 16 h. Morphometric analyses were performed as previously reported (17).

Neuroprotection Assay. Hippocampal neurons were preincubated with 1.2 μM STI1 for 1 h, followed by the addition of 25 nM staurosporine for 16 h. Signaling inhibitors were incubated 1 h before the addition of STI1. Cell death was estimated as the percentage of cells showing pyknotic nuclei (17).

Prion Infection. The N2a mouse neuroblastoma clone 5 cell line and SN56 cells were infected with 1% brain homogenate from a terminally sick 22L prion strain–infected C57BL/6 mouse or with brain homogenate from a non-infected mouse (44). Mock and 22L-infected cells were equally passaged and maintained to avoid any clonal effect. For the exposure of primary neurons to scrapie-infected brain, neuronal cultures from E17 mice were prepared and exposed to 0.1% 22L prion-infected brain homogenate or to brain homogenate from an uninfected mouse. At 24 h postexposure, the medium was filtered to remove debris. Cells were assayed for PrP^C and PrP^{Sc} content as previously described (44).

ACKNOWLEDGMENTS. This work was supported by Fundação de Amparo à Pesquisa do Estado de São Paulo (FAPESP) Grants 2008/00390 (to G.N.M.H.), 2002/12597-7, 2003-13189-2 (to V.R.M.), and 2008/53119-7 (to B.A.C.) and by Programa Institutos Nacionais de Ciência e Tecnologia, Conselho Nacional de Desenvolvimento Científico e Tecnológico (CNPq/MCT). FAPESP fellowships (to M.R. and F.H.B.) and a Conselho Nacional de Desenvolvimento Científico e Tecnológico (CNPq) fellowship (to G.L.M.) are gratefully acknowledged. V. R.M. is an International Scholar of the Howard Hughes Medical Institute.

1. Aguzzi A, Sigurdson C, Heikenwaelder M (2008) Molecular mechanisms of prion pathogenesis. *Annu Rev Pathol* 3:11–40.
2. Linden R, et al. (2008) Physiology of the prion protein. *Physiol Rev* 88:673–728.
3. Klann E, Sweatt JD (2008) Altered protein synthesis is a trigger for long-term memory formation. *Neurobiol Learn Mem* 89:247–259.
4. Kandel ER (2001) The molecular biology of memory storage: a dialogue between genes and synapses. *Science* 294:1030–1038.
5. Mathews M, Sonenberg N, Hershey J (2006) *Translational Control in Biology and Medicine* (Cold Spring Harbor Laboratory Press, Cold Spring Harbor).
6. Klann E, Dever TE (2004) Biochemical mechanisms for translational regulation in synaptic plasticity. *Nat Rev Neurosci* 5:931–942.
7. Jastrzebski K, Hannan KM, Tchoubrieva EB, Hannan RD, Pearson RB (2007) Coordinate regulation of ribosome biogenesis and function by the ribosomal protein S6 kinase, a key mediator of mTOR function. *Growth Factors* 25:209–226.
8. Raught B, et al. (2004) Phosphorylation of eucaryotic translation initiation factor 4B Ser422 is modulated by S6 kinases. *EMBO J* 23:1761–1769.
9. Dorrello NV, et al. (2006) S6K1- and betaTRCP-mediated degradation of PDCD4 promotes protein translation and cell growth. *Science* 314:467–471.
10. Cammalleri M, et al. (2003) Time-restricted role for dendritic activation of the mTOR-p70S6K pathway in the induction of late-phase long-term potentiation in the CA1. *Proc Natl Acad Sci USA* 100:14368–14373.
11. Kelleher RJ, 3rd, Govindarajan A, Tonegawa S (2004) Translational regulatory mechanisms in persistent forms of synaptic plasticity. *Neuron* 44:59–73.
12. Banko JL, et al. (2005) The translation repressor 4E-BP2 is critical for eIF4F complex formation, synaptic plasticity, and memory in the hippocampus. *J Neurosci* 25:9581–9590.
13. Costa-Mattioli M, et al. (2005) Translational control of hippocampal synaptic plasticity and memory by the eIF2alpha kinase GCN2. *Nature* 436:1166–1173.
14. Martins VR, et al. (2009) Prion Protein: Orchestrating Neurotrophic Activities. *Curr Issues Mol Biol* 12:63–86.
15. Lima FR, et al. (2007) Cellular prion protein expression in astrocytes modulates neuronal survival and differentiation. *J Neurochem* 103:2164–2176.
16. Coitinho AS, et al. (2007) Short-term memory formation and long-term memory consolidation are enhanced by cellular prion association to stress-inducible protein 1. *Neurobiol Dis* 26:282–290.
17. Lopes MH, et al. (2005) Interaction of cellular prion and stress-inducible protein 1 promotes neuritogenesis and neuroprotection by distinct signaling pathways. *J Neurosci* 25:11330–11339.
18. Waskiewicz AJ, et al. (1999) Phosphorylation of the cap-binding protein eukaryotic translation initiation factor 4E by protein kinase Mnk1 in vivo. *Mol Cell Biol* 19: 1871–1880.
19. Swiech L, Perycz M, Malik A, Jaworski J (2008) Role of mTOR in physiology and pathology of the nervous system. *Biochim Biophys Acta* 1784:116–132.
20. Hetz C, Russelakis-Carneiro M, Maundrell K, Castilla J, Soto C (2003) Caspase-12 and endoplasmic reticulum stress mediate neurotoxicity of pathological prion protein. *EMBO J* 22:5435–5445.
21. Ito T, Yang M, May WS (1999) RAX, a cellular activator for double-stranded RNA-dependent protein kinase during stress signaling. *J Biol Chem* 274:15427–15432.
22. Sim VL, Caughey B (2009) Recent advances in prion chemotherapeutics. *Infect Disord Drug Targets* 9:81–91.
23. Leung KM, et al. (2006) Asymmetrical beta-actin mRNA translation in growth cones mediates attractive turning to netrin-1. *Nat Neurosci* 9:1247–1256.
24. Morita T, Sobue K (2009) Specification of neuronal polarity regulated by local translation of CRMP2 and tau via the mTOR-p70S6K pathway. *J Biol Chem* 284:27734–27745.
25. Wendel HG, et al. (2007) Dissecting eIF4E action in tumorigenesis. *Genes Dev* 21: 3232–3237.
26. Anjum R, Blenis J (2008) The RSK family of kinases: Emerging roles in cellular signalling. *Nat Rev Mol Cell Biol* 9:747–758.
27. Shahbazian D, et al. (2006) The mTOR/PI3K and MAPK pathways converge on eIF4B to control its phosphorylation and activity. *EMBO J* 25:2781–2791.
28. Grider MH, Park D, Spencer DM, Shine HD (2009) Lipid raft-targeted Akt promotes axonal branching and growth cone expansion via mTOR and Rac1, respectively. *J Neurosci Res* 87:3033–3042.
29. Di Nardo AA, et al. (2007) Dendritic localization and activity-dependent translation of Engrailed1 transcription factor. *Mol Cell Neurosci* 35:230–236.
30. Pastor MD, et al. (2009) mTOR/S6 kinase pathway contributes to astrocyte survival to ischemia. *J Biol Chem* 284:22067–22078.
31. O'Driscoll C, Wallace D, Cotter TG (2007) bFGF promotes photoreceptor cell survival in vitro by PKA-mediated inactivation of glycogen synthase kinase 3beta and CREB-dependent Bcl-2 up-regulation. *J Neurochem* 103:860–870.
32. De Gregorio G, et al. (2007) The p85 regulatory subunit of PI3K mediates TSH-cAMP-PKA growth and survival signals. *Oncogene* 26:2039–2047.
33. Costa-Mattioli M, Sossin WS, Klann E, Sonenberg N (2009) Translational control of long-lasting synaptic plasticity and memory. *Neuron* 61:10–26.
34. Takei N, et al. (2004) Brain-derived neurotrophic factor induces mammalian target of rapamycin-dependent local activation of translation machinery and protein synthesis in neuronal dendrites. *J Neurosci* 24:9760–9769.
35. Huang F, Chotiner JK, Steward O (2005) The mRNA for elongation factor 1alpha is localized in dendrites and translated in response to treatments that induce long-term depression. *J Neurosci* 25:7199–7209.
36. Cox LJ, Hengst U, Gurskaya NG, Lukyanov KA, Jaffrey SR (2008) Intra-axonal translation and retrograde trafficking of CREB promotes neuronal survival. *Nat Cell Biol* 10:149–159.
37. McLennan NF, et al. (2004) Prion protein accumulation and neuroprotection in hypoxic brain damage. *Am J Pathol* 165:227–235.
38. Dunlop EA, Tee AR (2009) Mammalian target of rapamycin complex 1: signalling inputs, substrates and feedback mechanisms. *Cell Signal* 21:827–835.
39. Goggin K, Beaudoin S, Grenier C, Brown AA, Roucou X (2008) Prion protein aggresomes are poly(A)+ ribonucleoprotein complexes that induce a PKR-mediated deficient cell stress response. *Biochim Biophys Acta* 1783:479–491.
40. Paquet C, et al. (2009) Neuronal phosphorylated RNA-dependent protein kinase in Creutzfeldt-Jakob disease. *J Neuropathol Exp Neurol* 68:190–198.
41. Paccalin M, et al. (2006) Activated mTOR and PKR kinases in lymphocytes correlate with memory and cognitive decline in Alzheimer's disease. *Dement Geriatr Cogn Disord* 22:320–326.
42. Chang RC, et al. (2002) Involvement of double-stranded RNA-dependent protein kinase and phosphorylation of eukaryotic initiation factor-2alpha in neuronal degeneration. *J Neurochem* 83:1215–1225.
43. Ertmer A, et al. (2004) The tyrosine kinase inhibitor STI571 induces cellular clearance of PrPSc in prion-infected cells. *J Biol Chem* 279:41918–41927.
44. Vorberg I, Raines A, Story B, Priola SA (2004) Susceptibility of common fibroblast cell lines to transmissible spongiform encephalopathy agents. *J Infect Dis* 189:431–439.